Solar Energy 252 (2023) 134–144

Contents lists available at ScienceDirect

Solar Energy

journal homepage: www.elsevier.com/locate/solener

Study of abrasion tests for antireflective and antisoiling/antireflective coatings on glass solar tubes

Gema San Vicente [a,*], Nuria Germán [a], Meryem Farchado [a], Ángel Morales [a], Patricia Santamaría [b], Aránzazu Fernández-García [c]

[a] CIEMAT-PSA, Materials for Concentrating Solar Thermal Technologies Unit, Avenida Complutense 40, Madrid 28040, Spain
[b] RIOGLASS Solar SCH, S.L., Parque de Actividades Medioambientales de Andalucía (PAMA), Ctra. Aznalcóllar - Gerena, Km. 1, P.O. Box 32, 41870, Aznalcóllar, Sevilla, Spain
[c] CIEMAT-PSA, Ctra Senés, Km. 4, P.O. Box 22, 04200 Tabernas, Almería, Spain

ARTICLE INFO

Keywords:
Antisoiling
Antireflective
Solar glass covers
Abrasion
Degradation mechanism

ABSTRACT

The abrasion resistance of the antireflective coatings (ARC) applied on both sides of the parabolic-trough glass tubes is a key point to maintain throughout time the enhanced efficiency which produces the use of this film. The cleaning processes as well as the erosion produced by dust or sand in desert environments can damage the ARC, even removing it, affecting the system efficiency. The use of an antisoiling (AS) treatment on the antireflective (AR) coated solar glass envelopes are reaching increasing interest to reduce soiling and the water consumption associated to cleaning. RIOGLASS AR coated tubular samples were coated with a commercial hydrophobic treatment and the abrasion resistance of the AR + AS coatings combination against sole ARC were studied by carrying out two abrasion tests. Initial average solar transmittance values of 96.9 % and initial average static contact angle of 107° were obtained for the AR + AS samples. The results from the two abrasion tests have shown that the AR + AS coatings combination present a higher resistance to the abrasion. It has also been observed that two different abrasive media in the sand oscillating test produce different degradation mechanisms, (reflection losses versus absorptance losses). Additionally, the results have shown that solar transmittance values are not enough to characterize the abrasion degradation of AR coatings, being also important the haze value. Similar solar transmittance values (93.9 % and 94 %) but with different haze values (1.2 % against 3.2 %) and very different transmittance spectra indicating distinct degradation mechanism were obtained for samples abraded with two different sands.

1. Introduction

The ability of the antireflective coating (ARC) applied on the glass covers of concentrated solar power (CSP) receivers to withstand abrasion, produced by sand or other airborne particles as well as cleaning processes to remove accumulated soiling, is fundamental to assure the efficiency increase obtained thanks to it. In fact, enhancing the abrasion-resistance of this kind of materials is attracting a great deal of interest (Chi et al., 2019; Joo et al., 2011; Khan et al., 2018; Li and He, 2017; Xia et al., 2014; Zhang et al., 2019). Furthermore, soiling processes in solar technologies imply financial losses due to the reduction in the optical efficiency as well as to the increase in operation and maintenance cost associated to cleaning. In the case of CSP, it has been reported that the financial losses produced by soiling were estimated to be between 70 M € and 100 M € in 2020 taking into consideration a global collector (aperture) area of around 40x106 m^2 (Ilse et al., 2019). Actually, although the dust deposition provokes losses in both solar energy technologies (photovoltaics (PV) and CSP), the impact produced in CSP is much more remarkable and therefore, more investigations in this topic are required (Zereg et al., 2022). Specifically, in (Bellmann et al., 2020) it was found that the optical soiling losses produced by soiling are higher by a factor of 8–14 in CSP with the same particle surface densities compared to PV. These numbers are also confirmed in (Abraim et al., 2022) where it was reported that the annual energy loss due to soiling is about 8 times higher for CSP than for PV, comparing the power production of both technology plants with the same capacity (1 MWe), in the same site (Morocco), and the same cleaning conditions. The interest in understanding soiling effect in solar technologies as well as in using

* Corresponding author.
E-mail address: gema.sanvicente@ciemat.es (G. San Vicente).

https://doi.org/10.1016/j.solener.2023.01.055
Received 19 September 2022; Received in revised form 18 January 2023; Accepted 30 January 2023
Available online 7 February 2023

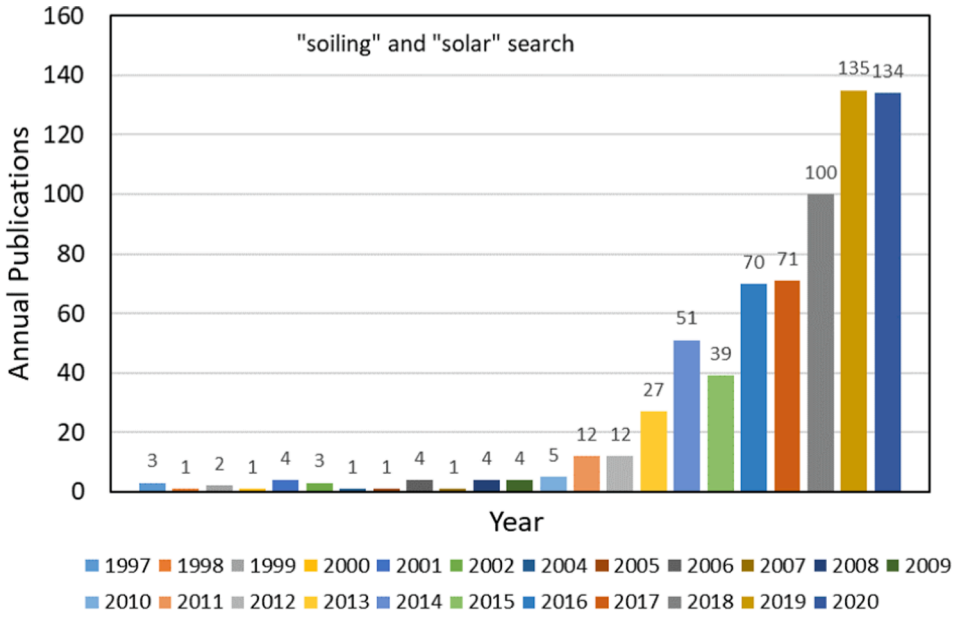

Fig. 1. Histogram of scientific publications per year obtained after executing a search in the Web of Science website with the topic "soiling" and "solar".

soiling mitigation strategies, as innovative highly efficient cleaning processes and the use of AS coatings, is growing exponentially since 2010. Fig. 1 represents the histogram of number of scientific publications per year obtained after executing a search in the Web of Science website with the topic "soiling" and "solar" (San Vicente, 2022).

Within the Horizon 2020 SOLWARIS project, the use of an AS treatment on the AR coated glass tubes of receivers has been studied to reduce the tubes soiling. With the use of the coating, the water consumption associated to cleaning as well as the erosion damage produced by cleaning processes would decrease due to the reduction in cleaning frequency. Two different AS strategies (hydrophobic versus hydrophilic) with different actuation mechanisms have been studied for solar applications (Sutha et al., 2017; Wang et al., 2021; Wette et al., 2019), but up to now, not consensus has been reached among scientists about which is the best strategy to minimize soiling effect (Huang et al., 2021). The application of any of them on the ARC is a challenging issue as it is usually accompanied by a decrease in the ARC porosity (Himcinschi et al., 2002) an then in an increase of the refractive index (San Vicente et al., 2012), resulting in a decrease of the high transmittance achieved by the ARC.

The ARC abrasion resistance is a combination of different factors (adhesion, hardness, flexibility and impact resistance) and each test method measures a different combination of these factors. In this sense, many different methods are available to test wear resistance but none is found to reproduce and have correlations with real situations (Figgis and Bermudez, 2021). Abrasion test methods include at least three categories of test: falling sand, forced sand impingement and machine abrasion (Miller et al., 2016). The first one would represent the damage caused at relatively low wind speeds, the second one allows to simulate the effects of infrequent by damaging sandstorms, where high wind speeds are present, and the third one is intended to simulate the effect of surface erosion that occurs during the field use. Some standards are available about these testing methods but applied to other industries as textile, automotive, construction, etc. In some cases the conditions are too aggressive and the uncoated glass is also damaged (Mahdaoui et al., 2003). For the photovoltaic (PV) industry, an International Electrotechnical Commission (IEC) abrasion test standard to evaluate the degradation of AS and/or AR coatings on glass covers has just been published (IEC 62788-7-3) and a great number of research works have also been published to support the developing of this standard, overall focused in abrasion produced by cleaning processes (Lange et al., 2020; Miller et al., 2018; Miller et al., 2020; Newkirk et al., 2021). However, for CSP technologies whose soiling–induced losses are remarkably greater than PV and for which cleaning issues are more important, there is no standard available yet to study and simulate the abrasion effects on AR and/or AR + AS coatings on glass covers caused by sand, sandstorms or other airborne particles as well as cleaning processes. Regarding testing CSP components, a guideline was recently published within STAGE-STE project about the test parameters for testing reflectors and absorbers to simulate abrasion in desert environment with forced sand machines (Wiesinger et al., 2017). In the same way, in the IEC Technical Specification (TS) 62862-3-3, a stationary abrasive resistance test is suggested to be done for testing the glass envelopes of solar thermal receivers (2020). This test does not reproduce the real exposure conditions since the abrasive used is a rubber eraser but it is well suited to compare materials. In this paper, we study the abrasion resistance of the AR + AS coatings combination against sole AR coating on borosilicate tubular samples by the abrasion test included in IEC TS 62862-3-3 and by an oscillating sand test using two different abrasive media. The effect of the AS hydrophobic coating on the properties and abrasion resistance is examined and the comparison between both abrasion tests carried out is shown. The antisoiling capacity of the AS coating used was previously studied by exposing samples outdoors at Plataforma Solar de Almería (Spain) during 11 months (San Vicente et al., 2020).

2. Experimental procedure

2.1. Sample preparation and characterization

Borosilicate glass tubes used to produce PTR® solar receivers (4 m long, 3 mm thickness and 125 mm diameter) were coated with the RIOGLASS sol–gel ARC on both sides. Since RIOGLASS SOLAR is currently the owner of SCHOTT's parabolic through receivers manufacturing line, its technology is applied in the manufacturing of these glass tubes. Then, curved samples around 10 cm side size were obtained by cutting the tubes and a commercial hydrophobic AS treatment (ClearShield Eco-System™) was applied by rubbing the area with a cotton cloth wetted with the commercial solution in the external side of some of them in order to compare their mechanical resistance. However, if the AS coating was applied on the commercial 4 m long glass tube, the method of application used would be spraying as it is the methodology recommended by the AS suppliers for big surfaces. Three replicas of each

Table 1
Summary of the properties of the two abrasive media used in the oscillating sand test.

Abrasive mediaTest	Alundum ZF12	Ouarzazate sand
Colour	Grey	Brown
Composition (% wt)	Al_2O_3(>50 %), ZrO_2(25–50 %), HFO_2 (<2.5 %)	SiO_2(>50 %), CaO(15–20 %), Al_2O_3 (10–20 %), Fe_2O_3 (<10 %)
Maximum particle size (mm)	1.5	0.5
Particle shape	Sharp edges	Rounded edges

sample type were tested in the same conditions to minimize errors. Hemispherical transmittance spectra of the samples were measured at the wavelength range of 300–2500 nm. The equipment used was a UV/VIS/NIR Perkin-Elmer LAMBDA 950 double beam spectrophotometer with a 150 mm diameter Spectralon® coated integrating sphere. The solar hemispherical transmittance ($\tau_{s,h}$) was calculated by averaging the transmittance data over the direct AM1.5 solar spectral irradiance given by the current standard ASTM G-173-03, following the IEC 62862-1-1 standard (2018) as it is expressed in equation (1). The variation in these values was used as degradation indicators.

$$\tau_{s,h}(300,2500) = \frac{\int_{300}^{2500} \tau_{\lambda,h}(\lambda) G_b(\lambda) d\lambda}{\int_{300}^{2500} G_b(\lambda) d\lambda} \quad (1)$$

where $\tau_{\lambda,h}(\lambda)$ is the spectral hemispherical transmittance measured and $G_b(\lambda)$ is the spectral direct solar irradiance.

Total haze (H) values were calculated from transmittance measurements according to IEC 62805-1 standard (2017) at the wavelength range of 300–2500 nm. This parameter quantifies the light flux transmitted that is deviated from the direction of the incident beam, this is, the scattering of the transmitted light. Water static contact angle (WCA) measurements were performed with a KSV CAM 200 instrument to evaluate the effect of the AS coating on the sample surface, and an average value from 5 drops per sample was obtained. A Leica DM4 M optical microscopy with image acquisition system and software for image analysis was used to characterize the possible damage produced in the surface of the samples by the abrasion tests. Moreover, wear tracks produced by abrasion tests were characterized by profilometry with a Dektak 150 Surface Profiler. Five linear scans of 0.5 mm length with the 2 μm diameter pin and a load of 1 mg were performed per sample. Average surface roughness (R_a), according to ISO 4287, was calculated being the data presented the mean values of five measurements per sample for each set of samples.

2.2. Abrasion tests

Two different abrasion tests have been carried out to study the abrasion resistance. One of them is included in IEC TS 62862-3-3 [7], and consists of rubbing the dry glass sample with an abrasive rubber (eraser material according to standard MIL-E12397). A Taber linear abrader model 5750 was the equipment used and the test conditions applied were those recorded in the IEC TS, i.e. load weight of 350 g, stroke length of 40 mm and speed of 7 cycles/min. The other abrasion test, performed with a Taber oscillating abrasion tester model 6160, consists in putting the sample through an abrasive medium with an oscillating movement. The test parameters selected were a stroke length of 150 mm and a speed of 100 cycles per minute. The positioning of the specimens was such that only the outer part was subject to abrasion (the upper side). Standardized Alundum® ZF-12 (used in a standardized abrasive test for eyeglasses lenses) and Ouarzazate (Morocco) sand with particle size lower than 500 μm act as abrasive media. Sand from Ouarzazate was selected as this site is a deserted location with frequent sand storms events and furthermore the largest CSP plant in the world (NOOR power plant) is located there. In addition, the different properties of both materials, in terms of composition, colour, particle size and particle shape will provide information on the effect of the abrasive medium used in the test. The properties of both abrasive media are summarized in Table 1. Moreover, Fig. 2 shows the photographs of the oscillating sand tester together with the two abrasive media used.

After applying a defined number of abrasion cycles, the samples were removed and fully characterized. Since this test is not included in any standard or technical specification applied to this component (glass envelopes for solar receivers) neither similar conditions have been found in the bibliography, the number of cycles at which the test was stopped to study the sample evolution was defined by the authors themselves. The samples were analyzed after every 20 cycles from 0 to 120 cycles, every 30 cycles from 120 to 300 cycles and every 50 cycles from 300 to 1400 cycles. It is important to highlight that before characterization, a rigorous cleaning method was applied. It consists of removing the residues (rubber, sand, etc) with compressed air, rinsing generously with distilled water and ethanol, drying with compressed air, then applying five cleaning cycles with ethanol and wipes and finally, drying again

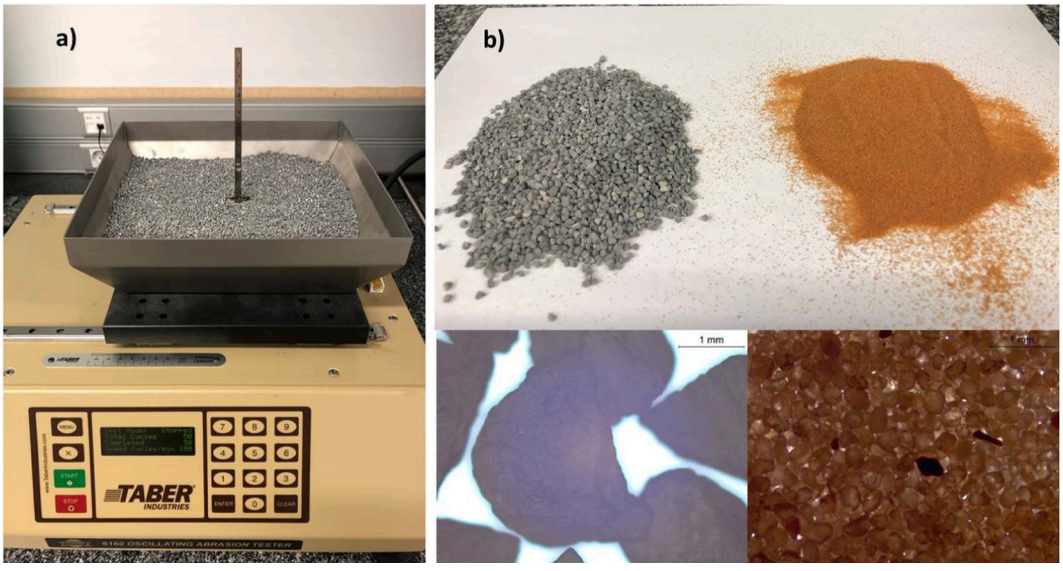

Fig. 2. Oscillating sand tester with the abrasive media used in the tests (standardized alundum® zf-12) (a) and photographs and microscope images of the two abrasives used (b).

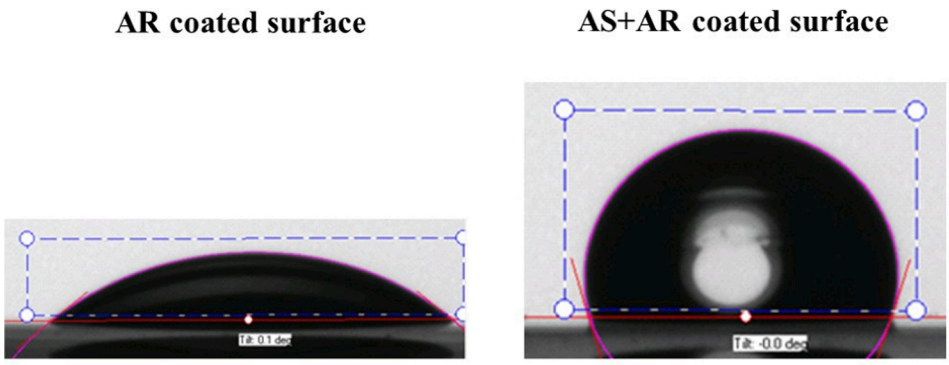

Fig. 3. Images of the water drop on the surface of the AR and AS + AR coated samples during the static contact angle measurements.

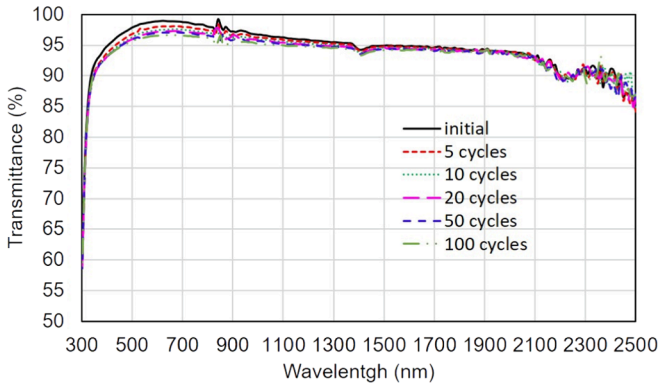

Fig. 4. Variation of the hemispherical transmittance spectra of one of the samples tested with Taber abrasion cycles.

with compressed air. This cleaning method is based on the best method reported by the authors Bruns et al., who studied different cleaning methods to assure a surface free of dusty residues after abrasion testing (Bruns et al., 2013).

3. Results and discussion

The solar transmittance values shown in all the figures and tables for all the samples are the average value from three measurements per sample and three replicas of each sample. 97.2 % is the average solar transmittance value for AR samples before testing and 96.9 % is the average solar transmittance value for AS + AR samples. When the AS coating is applied, a slight decrease in the solar transmittance value is produced and the surface wettability is modified. In fact, the surface static contact angle increases from an average value of 35.7° to 107.4°. Fig. 3 shows the images of a water drop on the surface of both types of samples.

3.1. Linear Taber test

This test is included in IEC TS 62862-3-3 as a suggested abrasion test for glass covers of CSP receivers. The conditions for testing are specified in the document but no pass/fail criterion is established. Fig. 4 displays the decrease of hemispherical transmittance with the number of abrasion cycles collected in the TS. Similar behaviour was observed in all samples tested (AR samples and AS/AR samples), although to different extents as shown below.

In Fig. 5 (a) it is shown the evolution of average solar transmittance calculated values as the average of samples of each set over the cycles performed. As it can be seen, from 20 abrasion cycles the solar transmittance values obtained from the average of AS treated samples are higher than the values obtained when the treatment was not applied. As the initial values for the AS treated samples were slightly lower than for the samples without it, the average solar transmittance values normalized to the initial mean value were calculated and the evolution over the rubbing cycles is also represented in Fig. 5 (b). This graphic clearly shows that the average of the samples with the AS hydrophobic treatment presents more resistance to the abrasion of the rubber than the average of the samples without this treatment from the first five abrasion cycles. These results are in accordance with those obtained by P. Santamaria et al. with a machine designed to perform the test under the IEC TS, though in the complete commercial tube, with similar samples (Santamaría et al., 2020). This improvement in the abrasion resistance produced by the hydrophobic treatment is attributed to a softer friction

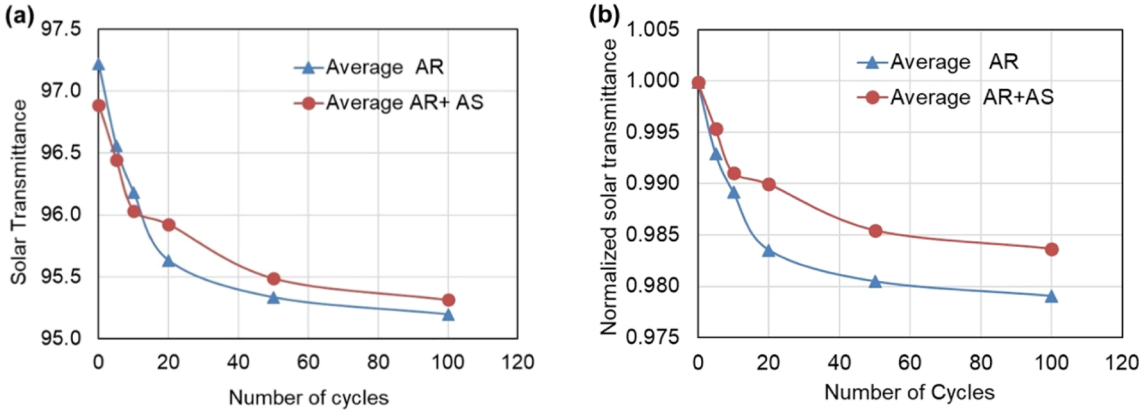

Fig. 5. Solar transmittance values (a) and normalized solar transmittance values (b) from average of each sample set vs abrasive rubbing cycles under IEC TS 62862-3-3 test conditions.

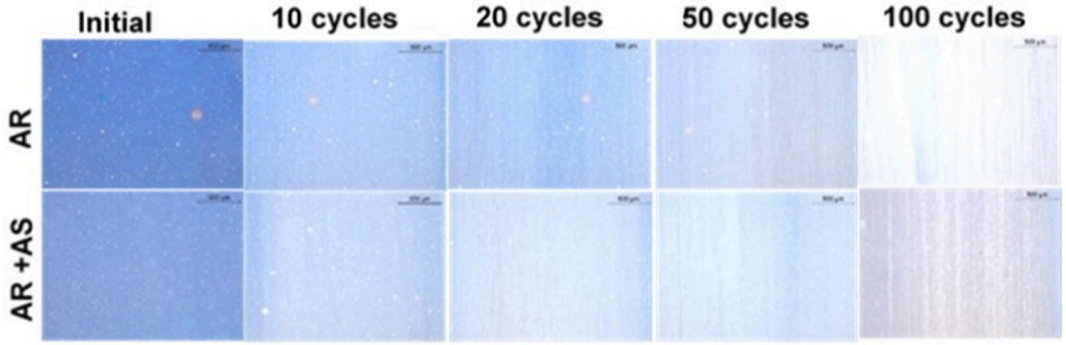

Fig. 6. Optical microscope images of an AR sample and an AS + AR sample before and after 10, 20 50 and 100 abrasion cycles. Magnification 50x.

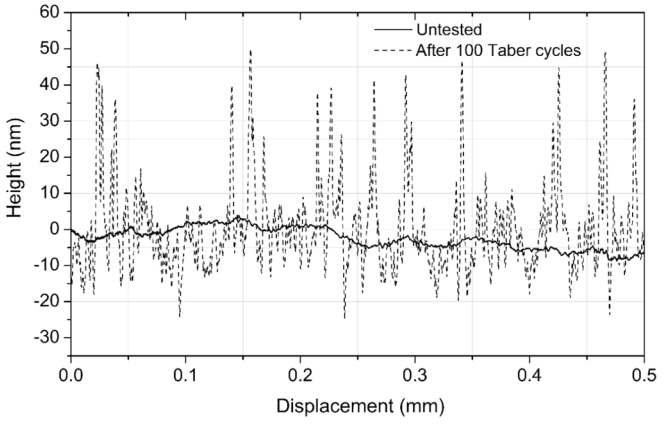

Fig. 7. 2D profile scan of AR sample before testing and after 100 Taber cycles.

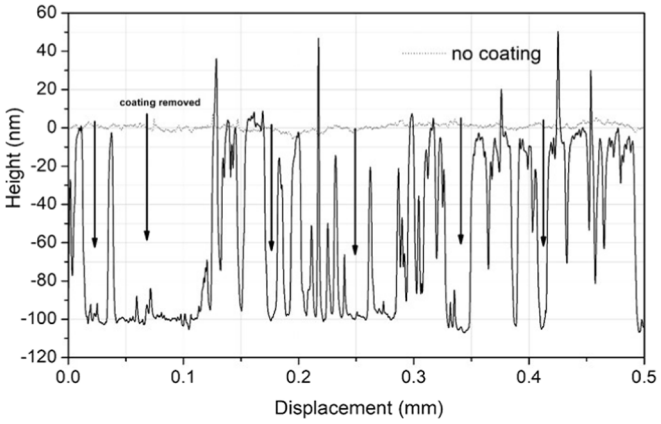

Fig. 8. 2D profile scan of AR sample with coating partially and completely removed after linear abrasion test.

between the abrasive rubber and the surface. The benefit of using this AS coating in abrasion resistance of the ARC was also previously demonstrated in two different types of abrasion tests: a forced sand chamber test (Wiesinger et al., 2018) and a combination of sand with wetted cleaning brushes test (San Vicente et al., 2018).

The microscope photos of one representative sample of each type before and after the abrasion cycles specified by the TS IEC 62862-3-3 are shown in Fig. 6. The scratches produced because of the abrasive action, which are not homogeneously distributed in the area abraded, can be observed in the microscope images. In addition to the scratches, the samples colour change with the number of cycles, indicating the removal and thinning of the coating. By comparing the photos of the samples with and without the AS treatment, it can be observed that the AS samples are more resistant to scratches and the surface is less damaged after the 100 cycles, as it was confirmed by the solar transmittance values decrease. Nevertheless, the complete removal of the AR coating after 100 abrasion cycles was not observed in any of the samples.

Average surface roughness values (Ra), obtained by different equipment such as atomic force microscopes (AFM) and stylus profilometers, are often used in abrasion research in AR coatings (Agea-Blanco et al., 2018; Agustín-Sáenz et al., 2020; Newkirk et al., 2021; Walls et al., 2022). Fig. 7 shows the profile scan of an AR sample before and after 100 linear abrasion cycles. Before testing, the AR sample profile is very smooth, with Ra values around 0.50 nm. Similar Ra values were obtained in the AS treated samples, showing no influence in this parameter. After testing, the scan presents a very different profile, with numerous hills and valleys that indicate the scratches produced in the coating by the rubber action. The Ra values after 100 abrasion cycles were between 8 nm and 12 nm. It should be noted that the vertical lengths between peaks and valleys are around 60–70 nm, showing no complete removal of the AR coating whose thickness is around 100 nm.

A higher number of linear abrasion cycles results in the profile are shown in Fig. 8. It can be seen areas where the coating has been removed, with vertical lengths around 100 nm. This profile presents a Ra value of 24.5 nm. The profile obtained when the coating is fully eliminated and then the stylus "see" the glass substrate is also plotted in Fig. 8. This profile is free of scratches and thus appears visually to un-abraded coating surface samples. In fact, Ra values are around 0.4–0.7 nm, similar to those obtained for the AR or AS/AR coating on the glass substrate. The similarity of an un-abraded sample and a completely abraded (removal of the coating) sample should be considered carefully to interpret the average roughness data. In conclusion, with this test conditions, it was found that the average roughness increases with the number of abrasion cycles as the coating becomes damaged and then decreases again as the coating is completely removed and the smooth glass substrate appears, being unaffected by the action of the abrasive. Newkirk et al. found similar variation in Ra values in AR coatings tested with different types of brushes to study their abrasion resistance (Newkirk et al., 2021).

3.2. Oscillating sand abrasion test

In this test, the abrasion is produced by the movement of different kind of sand unlike the previous test where the abrasion was produced by a rubber in movement. Two types of sand were employed in this study. On one hand, Alundum® ZF-12 is a standardized abrasive medium used commonly with this abrasion machine and it is composed by fused alumina–zirconia grains of around 1–2 mm size with sharp edges. On the other hand, the Ouarzazate sand is composed mainly by SiO_2 followed by alumina and lime (Fernández-García et al., 2018). This sand, sifted through a sieve to impose a maximum particle size of 500 μm is formed by particles with round edges (see microscope photos in Fig. 2). The choice of this particle size of 500 μm is based on information

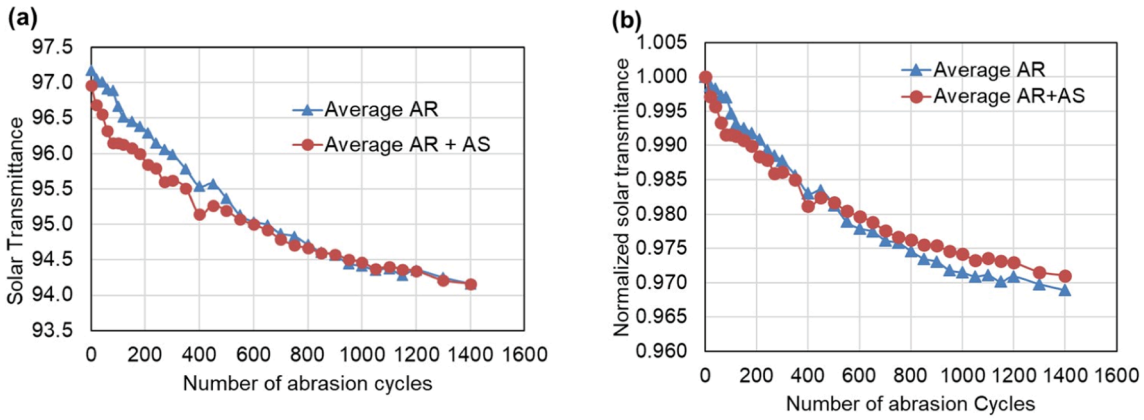

Fig. 9. Solar transmittance values (a) and normalized solar transmittance values (b) from average of each sample set vs abrasion cycles in the oscillating sand test with Alundum®.

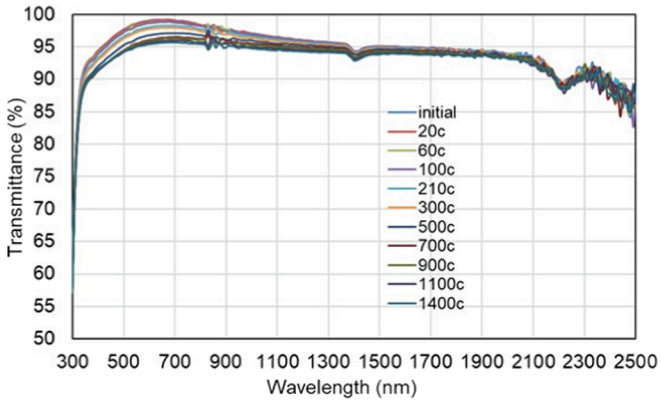

Fig. 10. Variation of the hemispherical transmittance spectra of one of the samples tested with the sand abrasion cycles using Alundum®.

found in literature that point out that the dust particles up to 1 mm can be lifted by strong wind and damage the surface, thus the use of particles >250 μm in laboratory erosion simulations is recommended (Sansom et al., 2017; Zereg et al., 2022). It was also previously reported that the morphology of the sand is crucial in the damage produced by erosion (Agea-Blanco et al., 2018).

Regarding the test performed with Alundum®, in Fig. 9 (a) the drop in the average solar transmittance values is plotted together with the drop in the values normalized to the initial value calculated as the average of samples of each set over the cycles (Fig. 9 (b)). The solar transmittance values show that the initial value is higher for the samples without the AS treatment, and comparing both types of samples, no higher solar transmittance values are obtained for the AR + AS samples during the test, and similar values are obtained after 1400 cycles of abrasion. However, comparing the normalized values, it can be seen that the drop in normalized solar transmittance values is lower when the AS coating is applied from 450 abrasion cycles, being the slope less pronounced.

In Fig. 10 it is shown the variation in the hemispherical transmittance spectra with the number of cycles for one sample tested. Given the high number of spectra, only the spectra obtained at some selected numbers of cycles are plotted although the solar transmittance values for all the cycles are displayed in Fig. 9. The hemispherical transmittance spectra shown are representative as all the samples presented similar behaviour. It can be seen that all the transmittance spectra follow the same (proportional) pattern with the abrasion cycles, being the same the shape of the curve with an only shift towards lower transmittance values in the 300–1500 nm wavelength range. These variations are similar to those obtained in the previous Linear Taber test (Fig. 4).

The degradation of coating samples throughout the test can be also observed in the optical microscope images of Fig. 11. Due to the great number of photos available, only some selected ones are shown here to facilitate the examination. The action of the abrasive sand of the surface is clearly seen in the images. Scratches similar to those observed with the rubber under EC TS 62862-3-3 were observed, although in this case, the microscope images show that the area damaged is more homogenous.

With respect to the samples tested with Ouarzazate sand, Fig. 12 shows the decrease in the average solar transmittance values and

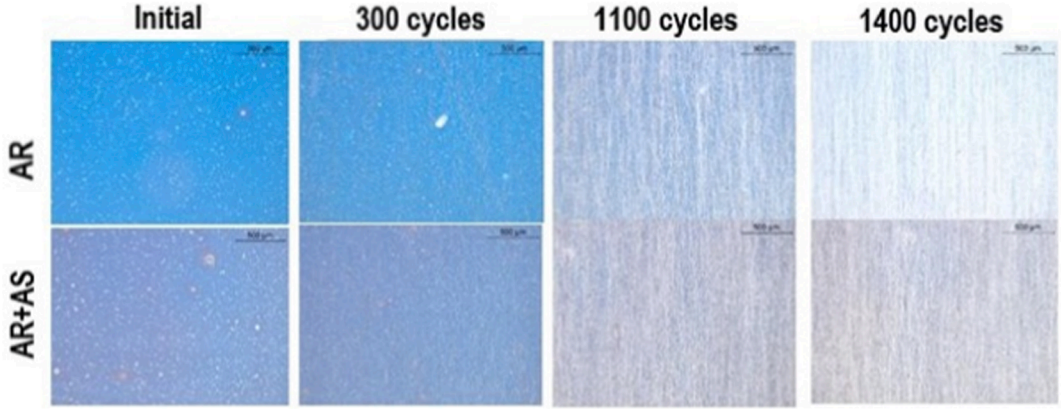

Fig. 11. Optical microscope images of representative AR coated and AS + AR coated samples before and after 300, 1100 and 1400 sand abrasion cycles with Alundum® ZF-12. Magnification 50×.

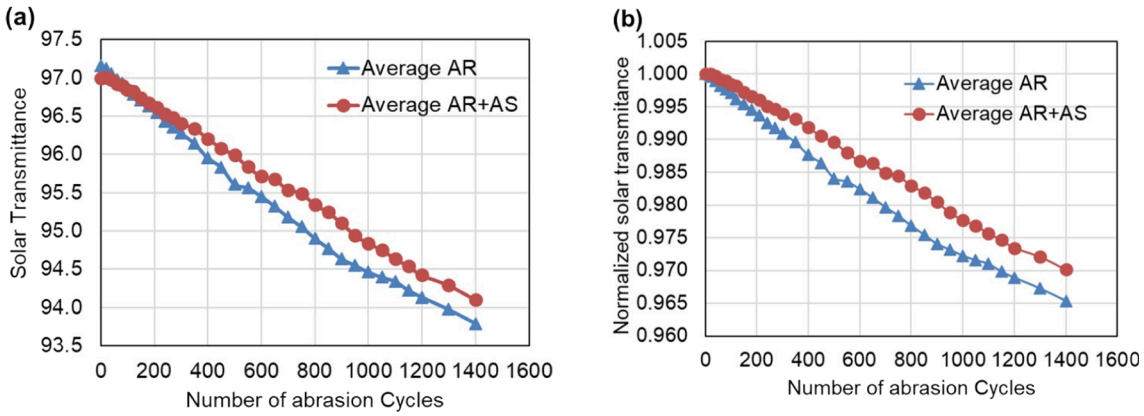

Fig. 12. Solar transmittance values (a) and normalized solar transmittance values (b) from average of each sample set vs abrasion cycles in the oscillating sand test with Ouarzazate sand 500 μm.

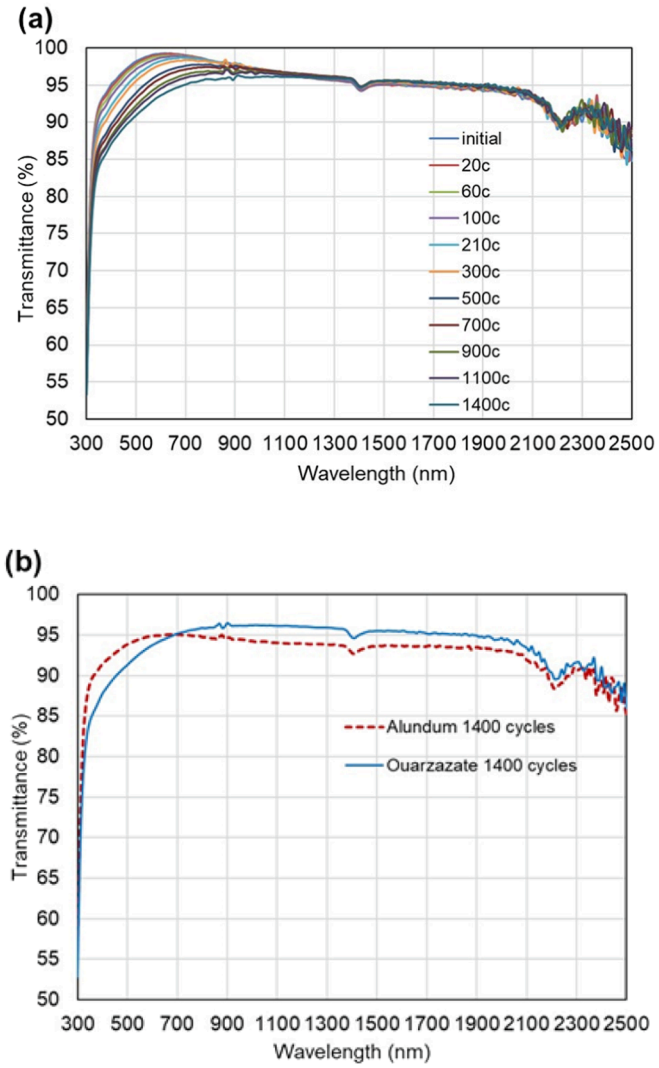

Fig. 13. Hemispherical transmittance spectra with the sand abrasion cycles using Ouarzazate sand (a) and comparison of transmittance spectra of samples tested during 1400 cycles with the two abrasive media used, Alundum® and Ouarzazate sand.(b).

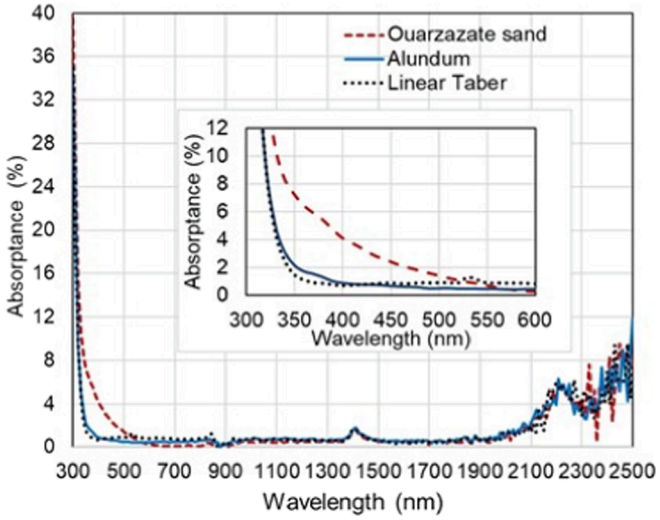

Fig. 14. Spectral absorptance of one sample tested in each type of abrasion test and an amplification of the wavelength zone were the differences are more detectable.

average normalized transmittance values of AS and AS + AR samples with the number of abrasion cycles. It should be noted that the decrease in solar transmittance and the following higher resistance to the sand abrasion is clearly shown for the samples with the AS treatment since the beginning (Fig. 12 (a)). As the initial values are lower for the samples with the AS treatment, this higher abrasion resistance was definitely exhibited since around 200 abrasion cycles, being the solar transmittance values higher than in the case of the AR coated samples. In the graphic with the normalized values (Fig. 12 (b)), the lower degradation of the AR + AS samples is clear from the first abrasion cycles.

Fig. 13 displays the evolution of transmittance spectra with the cycles for a representative sample tested with Ouarzazate sand (a) together with the transmittance spectra of two samples tested the same number of cycles (1400) with the two abrasive media. Regarding the transmittance evolution, it should be emphasized that the variation in the spectra with the abrasion cycles when Ouarzazate sand was used is different to the variation observed when the abrasive media was Alundum®. For the last ones, the transmittance decreases evenly, whereas in the samples tested with Ouarzazate sand, the variation is sharper at lower wavelength. The difference can be seen clearer in Fig. 13 (b). The same behaviour was observed for all the samples tested in the same conditions, both in AR and AR + AS samples. It is remarkable that both plotted samples have similar solar transmittance values (93.9 % for the sample tested with Alundum® as abrasive medium and 94 % for the sample tested with Ouarzazate sand as abrasive medium).

Taking into account these results, similar flat coated glass samples

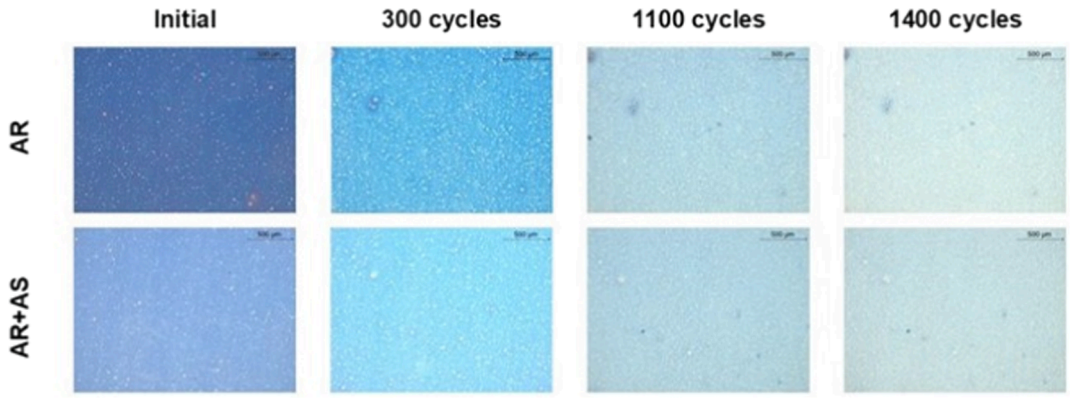

Fig. 15. Optical microscope images of representative AR coated and AS + AR coated samples before and after 300, 1100 and 1400 sand abrasion cycles with Ouarzazate sand. Magnification 50×.

were prepared and tested in the same abrasion conditions, in order to measure the hemispherical reflectance spectra and calculate the spectral absorptance according to the next equation:

$$\alpha_\lambda = 1 - \tau_{\lambda,h} - \rho_{\lambda,h} \quad (2)$$

where $\tau_{\lambda,h}$ is the spectral hemispherical transmittance and $\rho_{\lambda,h}$ is the spectral hemispherical reflectance.

The spectral absorptance obtained for one sample tested in each type of abrasion test is represented in Fig. 14.

The graph shows that the absorptance spectra are similar and practically zero in the whole wavelength range for the samples tested with the linear Taber test and the oscillating sand abrasion test with Alundum®. However, in the case of the sample tested with Ouarzazate sand, the absorptance increased at 300–600 nm wavelength range, which is the range where an anomalous transmittance decrease was observed (Fig. 13 left). Therefore, it can be said that the Ouarzazate sand damage produces a decrease in transmittance not for reflection increase, due to AR coating or AS + AR coatings removal, but also for an increase of absorptance in the sample, probably produced by the glass texturing and/or the presence of light trapping sand particle embedded in the glass. Furthermore, the total haze of both samples after 1400 cycles with the oscillating sand tester was calculated according to standard IEC 62805-1 (2017). The sample tested with Alundum® had a total haze value of 1.2 % while the sample tested with Ouarzazate sand had a total haze value of 3.2 %. Differences in the haze values by using different abrasive media with a sand oscillating tester were also reported by other authors (Bruns et al., 2013). Therefore, the abrasion with Ouarzazate sand not only produced absorption but also the transmitted radiation was more diffused than those transmitted when the sample is abraded with Alundum®. This is also an aspect to consider as the scattered radiation could not reach the absorber tube properly. The different behaviour obtained with the two abrasive media used is confirmed by the optical microscope photos (Fig. 15). As it can be seen in the figure, the Ouarzazate sand produced degradation by pitting more than scratches. Moreover, a whitening of the coatings was produced with the cycles and, in fact, the microscope lighting had to be decreased from 700 abrasion cycles to see clearly the contrast for this surface lightening. This response was observed in all the samples tested with this sand, with and without the AS coating. Thus, it confirms that the Ouarzazate sand damage produced the creation of a texture in the surface, which lead to a decrease in the transmittance because of an increase of absorptance in addition to producing scattering of the transmitted radiation. On the contrary, Alundum® material produced scratches in the coatings, being the decrease in transmittance caused by reflection losses produced by the elimination of the AR coating in some zones.

Fig. 16 shows the 2D profiles of two AR coated samples after 1400 abrasion cycles with the two abrasive media used. Both profiles present narrow peaks and valleys of different heights but important differences are observed between them. In the samples tested with Ouarzazate sand, an average value of total height of profile (R_t), which is the sum of height of the largest peak height and the largest valley depth, of 200 nm was achieved. However, the average Rt value for the samples tested with Alundum® was 100 nm. Similarly, the mean Ra value obtained from the profiles obtained with Ouarzazate sand was 21.8 nm whereas the mean Ra value when Alundum® was the abrasive material was practically half (9.3 nm). No remarkable differences between the values obtained for samples with or without AS treatment were obtained. The summary of the Ra and Rt values obtained in the samples tested in the three abrasion test is recorded in Table 2.

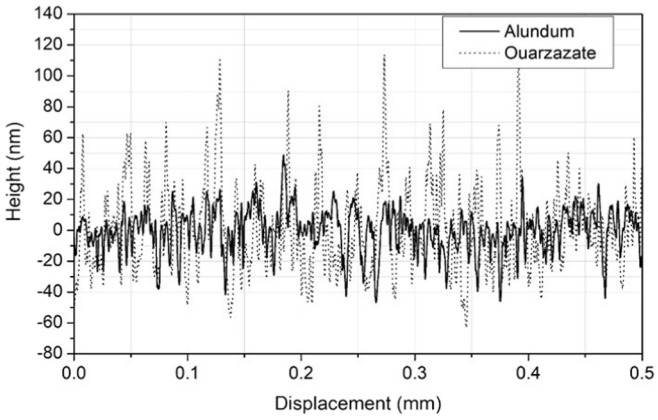

Fig. 16. 2D profile scan of AR coated samples after 1400 abrasion cycles with Alundum® and Ouarzazate sand.

Table 2
Summary of the average values obtained from profilometric measurements of all samples tested.

Test	Mean Ra (nm)	Mean Rt (nm)
Linear Taber	10.3	75
Oscillating Taber (Ourzazate sand)	21.8	200
Oscillating Taber (Alundum® sand)	9.3	100

The profiles obtained with the oscillating sand test, with such deep hills and valleys, suggest that the abrasive sand is also affecting the bare borosilicate glass. Subsequently, flat uncoated borosilicate glass were tested in the same conditions by using the two sands to provide support to this. Fig. 17 shows the comparison of the optical microscope images of AR coated borosilicate glass samples and uncoated borosilicate glass samples tested with the two abrasive media in the same conditions. It

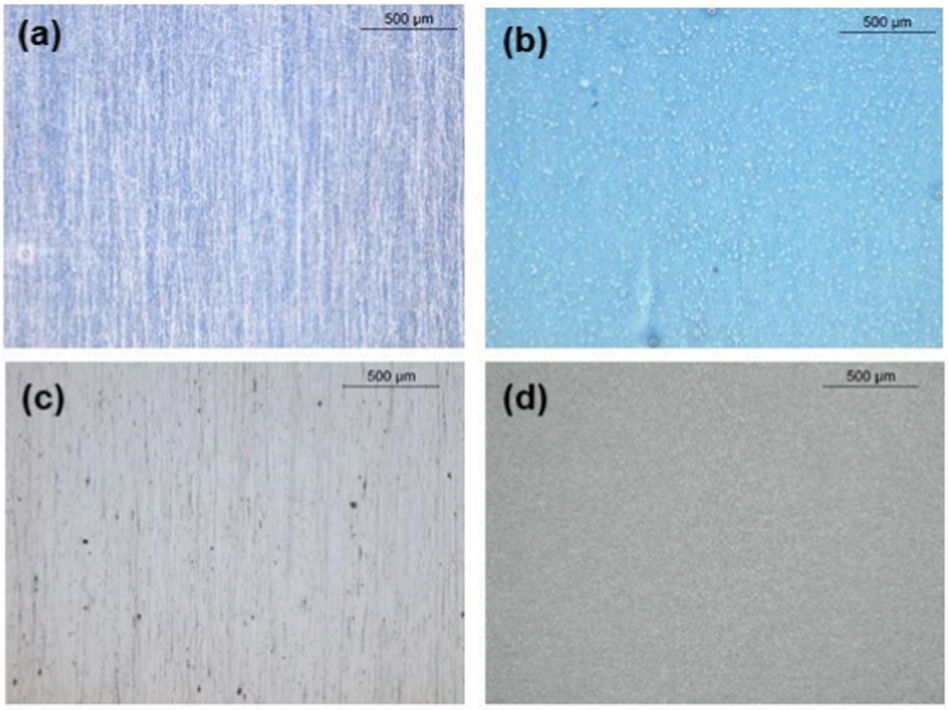

Fig. 17. Optical microscope images of AR coated borosilicate samples after 1000 abrasion cycles with Alundum® (a) and Ouarzazate sand (b) and of uncoated borosilicate glass tested in the same conditions with Alundum® (c) and Ouarzazate sand (d). Magnification 50×.

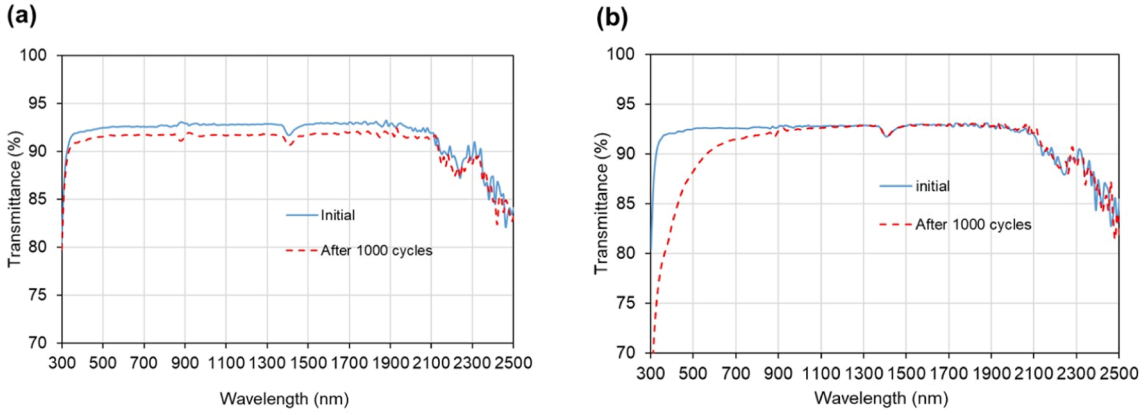

Fig. 18. Transmittance spectra of uncoated borosilicate glass samples before and after being tested with Alundum® as abrasive media (a) and Ouarzazate sand as abrasive media (b).

can be clearly seen the different damage caused by the two abrasives. The images of the AR coated samples have the characteristic blue colour that indicate the presence of the AR coating. The images of the uncoated glass samples, although colourless, clearly show the abrasion marks produced by the two types of sand, similar to those produced in the AR coated samples. Alundum® sand causes clean scratches while Ouarzazate sand causes pitting on both coated and uncoated glass, demonstrating that this test, under the conditions tested, also produce damage to the glass.

The transmittance spectra of the uncoated borosilicate glass samples before and after the abrasion test with both abrasive sands are shown in Fig. 18 and the calculated optical parameters are summarized in Table 2. The spectra shows that the borosilicate glass transmittance decreased after testing as it can be also seen in the $\tau_{s,h}$ values. Therefore, unlike the conditions used in the linear taber test, the oscillating sand test degraded the borosilicate glass substrate under the tested conditions. In addition, the differences in the spectra with the abrasive media used, are similar to those obtained in the AR and AS + AR coated samples. The glass sample tested with Ouarzazate sand has a solar transmittance value lower than the glass sample tested with Alundum (90.5 % vs 91.2 %), although the transmittance did not decrease after testing from 900 nm. This is because most of the energy in the solar spectrum is concentrated in the area where the transmittance decreases more for the sand abrasion.

Table 3
Calculated optical parameters and Ra measurements of uncoated glass samples before and after 1000 abrasion cycles with the two types of sand.

	$\tau_{s,h}$ (%)	H (%)	$\rho_{s,h}$ (%)	α_s (%)	Ra (nm)
Glass untested	92.4	0.0	7.7	0.0	0.3
Glass tested Alundum®	91.2	1.0	8.2	0.6	2.1
Glass tested Ourzazate	90.5	20.6	7.4	2.4	11.2

It is remarkable the differences obtained in the haze values and the solar absorptance values (Table 3). These differences are clearly related

to the abrasive medium and its properties because the destruction mechanism of the surface is different (as the microscope images and the transmittance spectra reveal). The optical degradation produced by Ouarzazate sand is mainly by an increase of scattering and absorption. This medium produces a texture that increases the surface roughness, leading to these phenomena. Moreover, the light-absorbing dust of this sand, may remain trapped in the pits in the glass or the coating, making it more difficult to remove completely and increasing the solar absorptance.With all these results, it should be remarked that "local" sands more than standarized sands should be used to test the abrasion resistance in laboratory tests.

4. Conclusions

The effect of applying a hydrophobic commercial AS coating on AR coated borosilicate samples in the abrasion resistance was studied. Two different abrasion equipments were used: a lineal Taber abraser with IEC TS 62862-3-3 and an oscillating abrasion sand machine with two different abrasive media. For the comparison of the methods, 18 samples were characterized by optical characterization and by microscopy analysis. The results showed that the use of this AS surface treatment on the AR coated borosilicate tubes clearly improved their mechanical resistance. Lineal Taber test and oscillating sand test using the standardized Alundum® material produced the same type of abrasion damage, clean scratches, decreasing the solar transmittance values mainly because of the reflection losses. However, the oscillating sand test with Ouarzazate sand as abrasive medium produced mechanical damage by pitting, creating a texture in the AR coating that lead to an increase of scattering and absorption in the sample. The oscillating sand test was a more aggressive test resulting in damage also to the borosilicate glass substrate, in the conditions of sand and speed used. The authors will study the application of softer parameters, as lower speed, to find conditions which will allow to characterize coatings without damaging the substrate. Under these conditions, it would be possible to compare the abrasion resistance of different coatings with the oscilating sand test, although it does not reproduce real operating conditions, as these are highly dependent on location and weather surroundings. Definitely, the two abrasive media used in the oscillating sand test showed different damage mechanisms that would not have been identified with the solar transmittance values as the only indicator of damage. Other optical parameters as haze and solar absoprtance are neccesary to complete the characterization of abraded coated glass samples. The results obtained showed that differences in haze values are correlated to the surface average roughness.

As a conclusion, not only the solar transmittance value should be considered to evaluate the abrasion resistant of AR coated glass samples but also the whole transmittance spectra and the spectral or total haze value. The use of profilometry scans in conjunction with optical microscope analysis and optical characterization is a valid characterization to study the abrasion of solar glass covers and to indentify the abrasion mechanisms.

Funding

This research received funding from the European Unionś H2020-LCE-2017-RES-IA research and innovation program under grant agreement number 792103, project SOLWARIS.

Declaration of Competing Interest

The authors declare that they have no known competing financial interests or personal relationships that could have appeared to influence the work reported in this paper.

Data availability

Data will be made available upon request to the authors.

References

Abraim, M., Salihi, M., El Alani, O., Hanrieder, N., Ghennioui, H., Ghennioui, A., El Ydrissi, M., Azouzoute, A., 2022. Techno-economic assessment of soiling losses in CSP and PV solar power plants: A case study for the semi-arid climate of Morocco. Energ. Conver. Manage. 270, 116285.

Agea-Blanco, B., Meyer, C., Müller, R., Günster, J., 2018. Sand erosion of solar glass: Specific energy uptake, total transmittance, and module efficiency. Int. J. Energy Res. 42 (3), 1298–1307.

Agustín-Sáenz, C., Machado, M., Nohava, J., Yurrita, N., Sanz, A., Brizuela, M., Zubillaga, O., Tercjak, A., 2020. Mechanical properties and field performance of hydrophobic antireflective sol-gel coatings on the cover glass of photovoltaic modules. Sol. Energy Mater. Sol. Cells 216, 110694.

Bellmann, P., Wolfertstetter, F., Conceição, R., Silva, H.G., 2020. Comparative modeling of optical soiling losses for CSP and PV energy systems. Sol. Energy 197, 229–237.

Bruns, S., Montzka, S., Reimann, W., Vergöhl, M., 2013. Comparison of abrasive tests for transparent optical coatings. Thin Solid Films 532, 73–78.

Chi, F., Liu, D., Wu, H., Lei, J., 2019. Mechanically robust and self-cleaning antireflection coatings from nanoscale binding of hydrophobic silica nanoparticles. Sol. Energy Mater. Sol. Cells 200, 109939.

Fernández-García, A., Juaidi, A., Sutter, F., Martínez-Arcos, L., Manzano-Agugliaro, F., 2018. Solar Reflector Materials Degradation Due to the Sand Deposited on the Backside Protective Paints. Energies 11, 808.

Figgis, B., Bermudez, V., 2021. PV coating abrasion by cleaning machines in desert environments – measurement techniques and test conditions. Sol. Energy 225, 252–258.

Himcinschi, C., Friedrich, M., Frühauf, S., I, S., Schulz, S., T, G., Baklanov, M., Mogilnikov, K., Zahn, D., 2002. Ellipsometric study of the change in the porosity of silica xerogels after chemical modification of the surface with hexamethyidisilazane. Anal. Bioanal. Chem. 374, 654–657.

Huang, Z.-S., Shen, C., Fan, L., Ye, X., Shi, X., Li, H., Zhang, Y., Lai, Y., Quan, Y.-Y., 2021. Experimental investigation of the anti-soiling performances of different wettability of transparent coatings: Superhydrophilic, hydrophilic, hydrophobic and superhydrophobic coatings. Sol. Energy Mater. Sol. Cells 225, 111053.

7. 2017. IEC 62805-1:2017. Method for measuring photovoltaic (PV) glass - Part 1: Measurement of total haze and spectral distribution of haze.

2018. IEC TS 62862-1-1:2018, Solar thermal electric plants - Part 1-1: Terminology.

2020. IEC TS 62862-3-3. SolarThermal Electric Plants - Part 3-3: Systems and Componentes - General Requirements andTest Methods for Solar Receivers.

Ilse, K., Micheli, L., Figgis, B.W., Lange, K., Daßler, D., Hanifi, H., Wolfertstetter, F., Naumann, V., Hagendorf, C., Gottschalg, R., Bagdahn, J., 2019. Techno-Economic Assessment of Soiling Losses and Mitigation Strategies for Solar Power Generation. Joule 3 (10), 2303–2321.

Joo, W., Kim, Y., Jang, S., Kim, J.K., 2011. Antireflection coating with enhanced anti-scratch property from nanoporous block copolymer template. Thin Solid Films 519 (11), 3804–3808.

Khan, S.B., Wu, H., Huai, X., Zou, S., Liu, Y., Zhang, Z., 2018. Mechanically robust antireflective coatings. Nano Res. 11 (3), 1699–1713.

Lange, K., Bahattab, M.A., Alqahtani, S.H., Mirza, M., Glaubitt, W., Naumann, V., Hagendorf, C., Ilse, K.K., 2020. Combined Soiling and Abrasion Testing of Antisoiling Coatings. IEEE J. Photovoltaics 10 (1), 243–249.

Li, T., He, J., 2017. Mechanically robust, humidity-resistant, thermally stable high performance antireflective thin films with reinforcing silicon phosphate centers. Sol. Energy Mater. Sol. Cells 170, 95–101.

Mahdaoui, T., Bouaouadja, N., Madjoubi, A., Bousbaa, C., 2003. Study of the Effects of Sand Blasting on Soda Lime Glass Erosion. Eng. J. Univ. Qatar 16, 125–138.

Miller, D.C., Einhorn, A., Lanaghan, C.L., Newkirk, J.M., To, B., Holsapple, D., Morse, J., Ndione, P.F., Moutinho, H.R., Alnuaimi, A., John, J.J., Simpson, L.J., Engtrakul, C., 2020. The abrasion of photovoltaic glass: A comparison of the effects of natural and artificial aging. IEEE J. Photovoltaics 10 (1), 173–180.

Miller, D.C., Muller, M.T., Simpson, L.J., 2016. Review of Artificial Abrasion Test Methods for PV Module Technology. NREL, pp. 1–20.

Miller, D.C., Einhorn, A., Engtrakul, C., Lanaghan, C., Micheli, L., Moutinho, H.R., Muller, M.T., To, B., Toth, S., Simpson, L.J., 2018. Soiling Related Abrasion and the Development of a PV Abrasion Standard, Conference: Presented at the International PV Soiling Workshop, 30 October - 1 November 2018, Golden, Colorado. United States, p. Medium: ED; Size: 11 MB.

Newkirk, J.M., Nayshevsky, I., Sinha, A., Law, A.M., Xu, Q., To, B., Ndione, P.F., Schelhas, L.T., Walls, J.M., Lyons, A.M., Miller, D.C., 2021. Artificial linear brush abrasion of coatings for photovoltaic module first-surfaces. Sol. Energy Mater. Sol. Cells 219, 110757.

San Vicente, G., Farchado, M., Germán, N., Morales, Á., 2018. Abrasion and Cleaning Tests on Antireflective and Antireflective/Antisoiling Coatings for Solar Glass Glazing, ISES Conference Proceedings. EuroSun 2018: 12th International Conference on Solar Energy and Buildings, Rapperswil, Switzerland, pp. 1–8.

San Vicente, G., Morales, A., Germán, N., Suarez, S., Sánchez, B., 2012. SiO_2/TiO_2 antireflective coatings with photocatalytic properties prepared by sol-gel for solar glass covers. J. Sol. Energy Eng. 134 (4), 041011–041011.

San Vicente, G., German, N., Maccari, A., Fernández-García, A., Morales, A., 2020. Soiling study on antireflective coated glass samples and antisoiling/antireflective coated glass samples. AIP Conf. Proc. 2303 (1), 210005.
San Vicente, G., 2022. ≤https://www.webofscience.com/wos/alldb/summary/06424286-f0a3-41aa-a76f-a8db9048b714-0fae95a7/relevance/1≥ (Accessed September 5th 2022.
Sansom, C., Almond, H., King, P., Endaya, E., Bouaichaoui, S., 2017. Airborne sand and dust soiling of solar collecting mirrors. AIP Conf. Proc. 1850 (1), 130011.
Santamaría, P., Domínguez, A., Rodríguez, M., Taravilla, S., 2020. Evaluation of optical properties and mechanical resistance of antisoiling layer on antireflective coated glass tubes for solar receivers, SOLARPACES. POSTER, Online event.
Sutha, S., Suresh, S., Raj, B., Ravi, K.R., 2017. Transparent alumina based superhydrophobic self–cleaning coatings for solar cell cover glass applications. Sol. Energy Mater. Sol. Cells 165, 128–137.
Walls, S.Y.E., Seda, S., Adam, L.A.W., John, M., 2022. Performance and durability of thin film solar cells via testing the abrasion resistance of broadband anti-reflection coatings. J. Energy Syst. 6 (1), 33–45.
Wang, P., Wang, H., Li, J., Ni, L., Wang, L., Xie, J., 2021. A superhydrophobic film of photovoltaic modules and self-cleaning performance. Sol. Energy 226, 92–99.
Wette, J., Fernández-García, A., Sutter, F., Buendía-Martínez, F., Argüelles-Arízcun, D., Azpitarte, I., Pérez, G., 2019. Water saving in CSP plants by a novel hydrophilic anti-soiling coating for solar reflectors. Coatings 9 (11), 739.
Wiesinger, F., King, P., Pagano, F., Bayon, R., Imbuluzqueta, G., Pescheux, A.-C., 2017. Report on the Methodology of Accelerated Erosion Testing for Reflectors and Absorbers. STAGE-STE PROJECT. Deliverable 8.5, pp. 1–11.
Wiesinger, F., San Vicente, G., Fernández-García, A., Sutter, F., Morales, Á., Pitz-Paal, R., 2018. Sandstorm erosion testing of anti-reflective glass coatings for solar energy applications. Sol. Energy Mater. Sol. Cells 179, 10–16.
Xia, B., Zhang, Q., Yao, S., Zhang, Y., Xiao, B., Jiang, B., 2014. Sol–gel silica antireflective coating with enhanced abrasion-resistance using polypropylene glycol as porogen. J. Sol-Gel Sci. Technol. 71 (2), 291–296.
Zereg, K., Gama, A., Aksas, M., Rathore, N., Yettou, F., Lal Panwar, N., 2022. Dust impact on concentrated solar power: A review. Environ. Eng. Res. 27 (6), 210345–1210340.
Zhang, J., Ai, L., Lin, S., Lan, P., Lu, Y., Dai, N., Tan, R., Fan, B., Song, W., 2019. Preparation of humidity, abrasion, and dust resistant antireflection coatings for photovoltaic modules via dual precursor modification and hybridization of hollow silica nanospheres. Sol. Energy Mater. Sol. Cells 192, 188–196.